Design and Simulation of Polarization-Independent Micro-Ring Resonator Based on Silicon Cross-Slot Waveguide Structure

Geng Minming[1,2,3,4]

[1]*School of Computer, Electronics and Information, Guangxi University, Nanning, Guangxi* 530004, *China*

[2]*Guangxi Key Laboratory of Multimedia Communications and Network Technology (Cultivating Base), Guangxi University, Nanning, Guangxi* 530004, *China*

[3]*Key Laboratory of Multimedia Communications and Information Processing of Guangxi Higher Education Institutes, Guangxi University, Nanning, Guangxi* 530004, *China*

[4]*Guangxi Experiment Center of Information Science, Guilin, Guangxi* 541004, *China*

Abstract Origin of polarization sensitivity of the silicon cross-slot waveguide (SCSW) is analyzed. The effective refractive indices as well as the single-mode-operation conditions of SCSWs for different polarization states are calculated. A single-mode SCSW can be polarization-insensitive if its structure is designed dedicated. A polarization-independent micro-ring resonator with 3.7 μm radius based on a polarization-insensitive SCSW is proposed and simulated. The polarization-independent working bandwidth of the micro-ring resonator is about 64 nm, and the free spectral range is about 35 nm.

Key words integrated optics; micro-ring resonator; cross-slot waveguide; polarization-independent; silicon-based waveguide

OCIS codes 230.3120; 230.3990; 230.4555; 230.7408

基于硅十字缝隙波导结构的偏振无关微环型谐振腔的设计与模拟

耿敏明[1,2,3,4]

[1]广西大学计算机与电子信息学院, 广西, 南宁 530004

[2]广西大学广西多媒体通信与网络技术重点实验室培育基地, 广西, 南宁 530004

[3]广西大学广西高校多媒体通信与信息处理重点实验室, 广西, 南宁 530004

[4]广西信息科学实验中心, 广西, 桂林 541004

摘要 分析了硅基十字缝隙波导(SCSW)偏振敏感的原因,计算了不同偏振态下SCSW的有效折射率和单模工作条件,分析发现通过合理的设计单模SCSW的结构,可以达到偏振不敏感。提出并模拟了基于SCSW的具有偏振无关特性的微环形谐振腔。该谐振腔的半径为3.7 μm,偏振无关的工作区域大约64 nm,自由光谱范围大约35 nm。

关键词 集成光学; 微环型谐振腔; 十字缝隙波导; 偏振无关; 硅基波导

中图分类号 TN256　　**文献标识码** A

doi: 10.3788/LOP53.022302

1 Introduction

The size reduction of integrated optical waveguide devices is one of the main concerns in photonics. The slot waveguide structure[1-2] is proposed to satisfy this demand. Since the polarization state of the optical signal transmitted in fiber is random, the spectral response of the optical devices used in fiber communication systems must be polarization-independent to make the systems stable. Several polarization-insensitive

收稿日期: 2015-07-01; **收到修改稿日期**: 2015-07-12; **网络出版日期**: 2015-12-30

基金项目: 广西大学科研基金项目(XJZ140261)、集成光电子学国家重点实验室开放课题(IOSKL2014KF13)

作者简介: 耿敏明(1981—),男,博士,讲师,主要从事集成光学、光网络、光滤波器、可重构光插分复用器等方面的研究。

E-mail: gengmm@gxu.edu.cn

schemes for different integrated optical devices have been proposed[3-7]. The structure of slot waveguide is quite asymmetric, which makes it polarization-sensitive. To solve this problem, cross-slot waveguide is introduced[8-9]. Several polarization-independent optical devices based on cross-slot waveguide structures have been proposed and fabricated[10-15].

The micro-ring resonator (MRR) based on high-index-contrast waveguide is one of the most attractive structures, which can construct various optical devices[16-18]. To the best of our knowledge, the polarization-independent MRR based on silicon cross-slot waveguide (SCSW) has not yet been proposed. In this paper, we report the design and simulation of a laterally coupled polarization-independent MRR based on SCSW. The fabrication of the MRR based on SCSW will be discussed in our following paper.

2 Design and simulation

2.1 Design of cross-slot waveguide

The polarization characteristic of integrated optical device heavily depends on the waveguide structure[19]. A single-mode SCSW with polarization-insensitive characteristic is required to design a polarization-independent MRR. The cross-section of a cross-slot waveguide based on silicon-on-insulator (SOI) is shown in figure 1. It consists of four rails of silicon separated by a slot of SiO_2. The SCSW is covered by SiO_2.

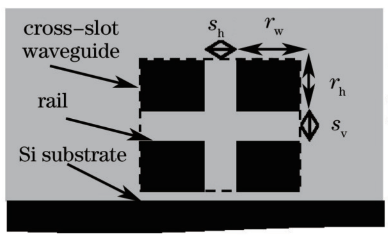

Fig.1 Cross-section of a cross-slot waveguide based on SOI

As shown in figure 1, there are four variables in this structure: r_w is the width of one rail, r_h is the height of one rail, s_h is the width of the slot between two rails in horizontal, and s_v is the height of the slot between two rails in vertical. To simplify the design of SCSW, the shapes of four rails are identical, and s_h is set equal to s_v. s_{hv} is used to denote both s_h and s_v.

Finite element method [20] is used to calculate the single-mode conditions and the effective refractive indices of different SCSWs for both TE and TM mode. At 1550 nm, the refractive index is 3.50 for Si and 1.44 for SiO_2. During the calculation process, r_w varies from 100 nm to 300 nm, and s_{hv} is set to be 50 nm and 100 nm respectively. Throughout this paper, the calculation grid sizes of three dimensions are all 10 nm. The single-mode-operation regions of SCSWs for both TE and TM mode are shown in figure 2.

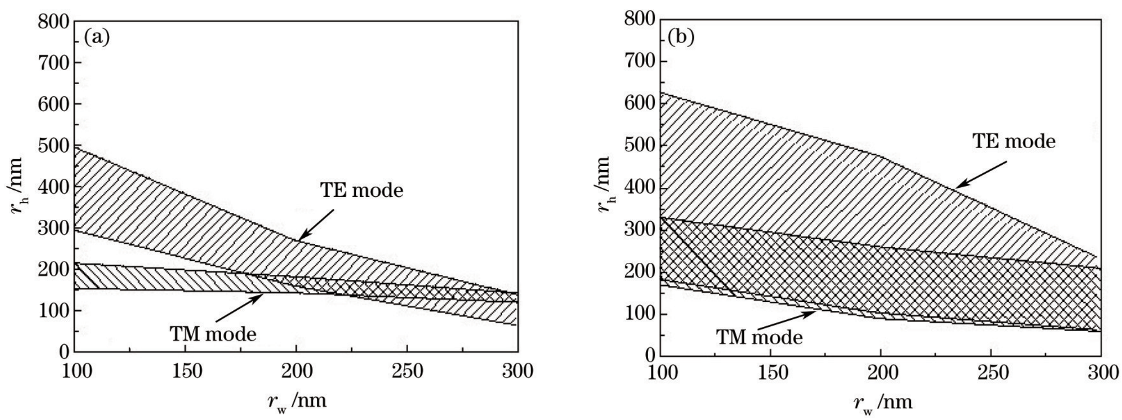

Fig.2 Single-mode-operation regions of SCSWs with different structural parameters for TE and TM mode.
(a) s_{hv} is 50 nm; (b) s_{hv} is 100 nm

The effective refractive indices of SCSWs with different structural parameters for both TE and TM mode are shown in figure 3.

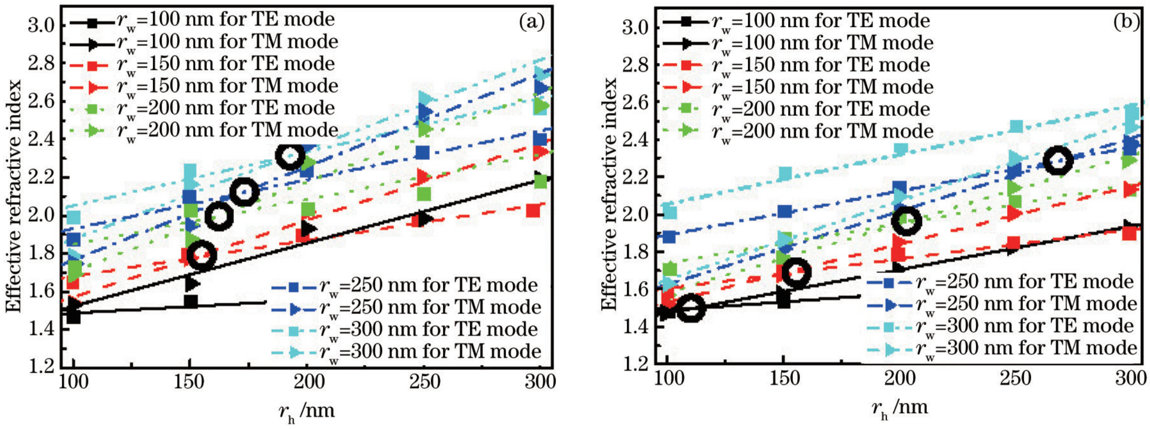

Fig.3 Effective refractive indices of SCSWs with different structural parameters for TE and TM mode. (a) s_{hv} equals to 50 nm; (b) s_{hv} equals to 100 nm

There are several intersections labeled by circles in figure 3, which mean the effective refractive indices for two polarization states are equal and the SCSWs with these structures are polarization-insensitive. We prefer s_{hv} to be 100 nm which can make the free spectral range (FSR) of the MRR larger. r_w and r_h are chosen to be 150 nm and 160 nm respectively, which can make the SCSW polarization-insensitive and satisfy the single-mode condition simultaneously. The effective refractive index is depend on the distribution of the optical field, which is the quantity of the light that passes through each point. The distributions of the optical field of different waveguide structures for TE mode are shown in figure 4. For a given polarization state, with the enlargement of s_{hv}, more optical field distributes in the slot with a low refractive index, which decreases the effective refractive indices. In contrast, with the enlargement of r_w or r_h, the optical field distributes in the four rails with high refractive index, which increases the effective refractive indices.

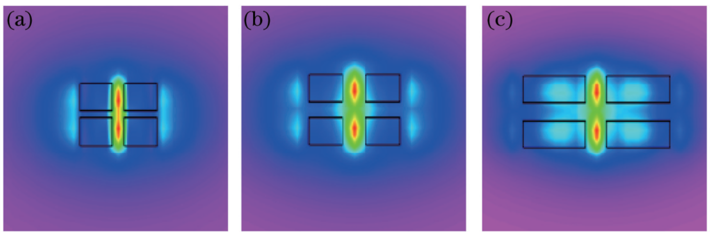

Fig.4 Distribution of the optical field for TE mode. (a) s_{hv} =50 nm, r_h =150 nm, r_w =150 nm; (b) s_{hv} =100 nm, r_h =150 nm, r_w =150 nm; (c) s_{hv} =100 nm, r_h =150 nm, r_w =300 nm

2.2 Design and simulation of micro-ring resonator

The top view of a MRR based on SCSW is shown in figure 5 (a). The MRR consists of a ring SCSW and two straight SCSWs. To cover the C-band which is used in fiber communication systems and ranging from 1530 nm to 1565 nm, the radius of the ring is set to be 3.7 μm. The cross-section of the coupling region is shown in figure 5 (b). The structure of the straight SCSW has been mentioned above. The structure of the ring SCSW is different. As shown in figure 5 (a), the four rails of the ring SCSW can be separated into two groups named inner rails and outer rails, each consists of two rails. To decrease the bending loss in the MRR[21], the width of the inner rails named r_{w_i} should be slightly larger than that of the outer rails named r_{w_o}. According to the analysis in reference 20, r_{w_i} and r_{w_o} are set to be 160 nm and 140 nm respectively.

The coupling coefficients of the MRR at 1550 nm for different polarization states with different gaps are calculated with three-dimensional finite-difference time-domain (FDTD) method[22-23] and the results are shown in figure 6. For a given gap, the coupling coefficients are different for TE and TM mode, which may make the filtering response of the MRR for TE and TM mode different. Scattering-matrix method[23-25]

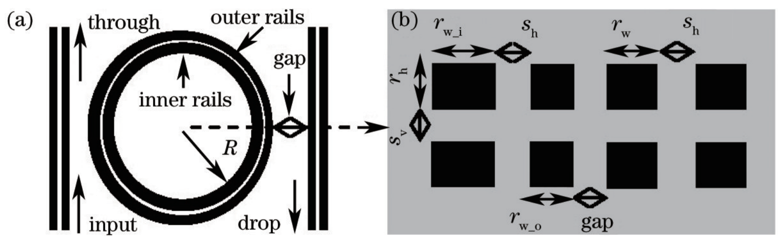

Fig.5 Structure of the MRR based on SCSW. (a) Top view of the MRR; (b) cross-section of the coupling region

is used to analyze the filtering performance of the MRR. According to the analysis in reference[23,26], the gap is set to be 320 nm to make the 3dB bandwidth of the MRR less than 0.8 nm.

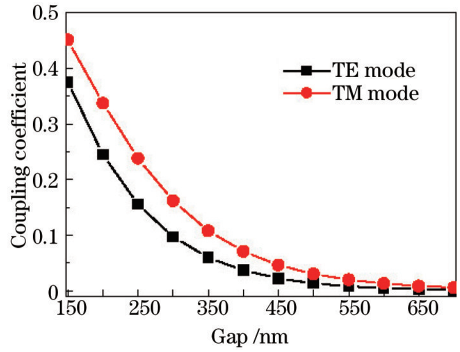

Fig.6 Coupling coefficients for two polarization states with different gaps

Three- dimensional FDTD method is used to analyze the filtering characteristics of the MRR with symmetric coupling structure. The main parameters used in the simulation are listed in table 1.

Table 1 Main parameters used in simulation

Parameter	Value
r_h /nm	160
r_w /nm	150
s_h /nm	100
s_v /nm	100
Gap /nm	320
R /μm	3.7
r_{w_i} /nm	160
r_{w_o} /nm	140

The simulation results are shown in figure 7. As shown, the line shapes for TE and TM mode are different, which is mainly caused by the different coupling coefficients for two polarization states. The resonant wavelengths for TE mode are 1463.98 nm, 1495.18 nm, 1528.89 nm and 1564.29 nm respectively, and those for TM mode are 1463.89 nm, 1495.20 nm, 1528.93 nm and 1564.86 nm respectively. The deviations of resonant

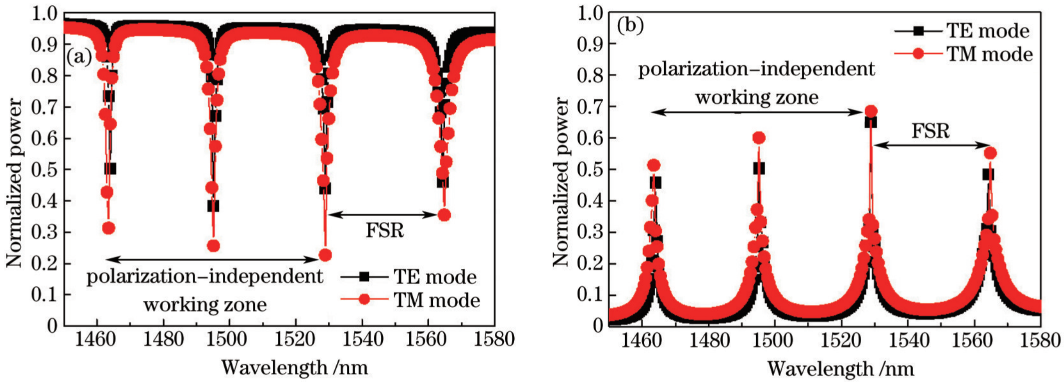

Fig.7 Response of the MRR simulated with three-dimensional FDTD method for TE and TM mode.
(a) At the through port; (b) at the drop port

wavelengths for two polarization states are less than 0.1 nm in the region of 1463 nm to 1529 nm, which is labeled as the polarization-independent working zone in figure 7. It means the polarization-independent working bandwidth of the MRR is about 64 nm, which is large enough to cover the C-band. The deviation tends to increase with the increase and decrease of wavelength, which is caused by the different dispersion characteristics for TE and TM mode. The FSR of the MRR is about 35 nm, which is large enough to avoid wavelength crosstalk in the dense wavelength division multiplexing (DWDM) systems.

At the through port, the 3 dB bandwidth at the resonant wavelength of about 1528 nm for TE mode is about 0.64 nm and TM mode about 0.77 nm. The Q values are calculated about 2387 and 1984 for TE and TM mode respectively:

$$Q = \lambda/\Delta\lambda_{3\,\mathrm{dB}} . \tag{1}$$

In equation (1), λ is the resonant wavelength, and $\Delta\lambda_{3dB}$ is the 3 dB bandwidth. The 3 dB bandwidths at the drop port for TE and TM mode are larger than 0.8 nm, which is mainly caused by the bending loss in the ring. The 3 dB bandwidth and Q value of the MRR can be optimized by adjusting the structure of SCSW or by decreasing the bending loss in MRR[21].

3 Conclusion

The design and simulation of a polarization-independent MRR based on SCSW structure are described. A single-mode SCSW can be polarization-insensitive if its structure is designed dedicated. The polarization-independent working bandwidth of the MRR is about 64 nm, which is large enough to cover the C-band. The polarization-independent working zone can be shifted to cover the C-band by optimization the structures of SCSW and MRR. The FSR of the MRR is about 35 nm which is large enough to be used in the DWDM systems.

References

1 Vilson R Almeida, Qianfan Xu, Carlos A Barrios, *et al*.. Guiding and confining light in void nanostructure[J]. Opt Lett, 2004, 29(11): 1209-1211.

2 Q F Xu, V R. Almeida, R R Panepucci, *et al*.. Experimental demonstration of guiding and confining light in nano-meter size low-refractive-index material[J]. Opt Lett, 2004, 29(14): 1626-1628.

3 Wenliang Wang, Xiaohong Rong. Double wavelength polarization insensitive beam splitter used in optical storage technology [J]. Chin Opt Lett, 2013, 11(S1): S10106.

4 Rui Zhang, Yufei Wang, Yejin Zhang, *et al*.. Broadband and polarization-insensitive subwavelength grating reflector for the near-infrared region[J]. Chin Opt Lett, 2014, 12(02): 020502.

5 Yin Xu, Jinbiao Xiao, Xiaohan Sun. Compact polarization beam splitter for silicon- based slot waveguides using an asymmetrical multimode waveguide[J]. J Lightwave Technol, 2014, 32(24): 4484-4490.

6 Md Faruque Hossain, Hau Ping Chan, Abbas Z Kouzani. Efficient design of polarization insensitive polymer optical waveguide devices considering stress-induced effects[J]. Opt Express, 2014, 22(8): 9334-9343.

7 Biswajeet Guha, Jaime Cardenas, Michal Lipson. Athermal silicon microring resonators with titanium oxide cladding[J]. Opt Express, 2013, 21(22): 26557-26563.

8 J V Galan, P Sanchis, J Garcia, *et al*.. Study of asymmetric silicon cross-slot waveguides for polarization diversity schemes [J]. Appl Opt, 2009, 48(14): 2693-2696.

9 A Khanna, A Saynatjoki, A. Tervonen, *et al*.. Non-birefringent cross-slot waveguide[C]. Proceeding of Laser and Electro-Optics and the European Quantum Electronics Conference, 2009.

10 Amit Khanna, Antti Säynätjoki, Ari Tervonen, *et al*.. Control of optical mode properties in cross-slot waveguides[J]. Appl Opt, 2009, 48(34): 6547-6552.

11 Xiaoguang Tu, Soo Seng Norman Ang, Ah Bian Chew, *et al*.. An ultracompact directional coupler based on gaas cross-slot waveguide[J]. IEEE Photon Technol Lett, 2010, 22(17): 1324-1326.

12 Matthieu Roussey, Petri Stenberg, Arijit Bera, *et al*.. Polarization independent integrated filter based on a cross-slot

waveguide[J]. Opt Express, 2014, 22(20): 24149-24159.

13 B M A Rahman, D M H Leung, N Kejalakshmy, *et al.*. Novel silicon cross-slot optical waveguide for polarization diversity applications[C]. Proceeding of Signal Processing in Photonic Communications Conference, 2013, JT3A: 22.

14 J V Galan, P Sanchis, J Garcia, *et al.*. Silicon cross-slot waveguides insensitive to polarization [C]. Proceeding of IEEE/LEOS Winter Topicals Meeting Series, 2009: 32-33.

15 Wanjun Wang, Haifeng Zhou, Jianyi Yang, *et al.*. Polarization-insensitive electro-optical modulator based on polymer-filled silicon cross-slot waveguide[C]. SPIE, 2009, 7630, 763016.

16 Wim Bogaerts, Peter De Heyn, Thomas Van Vaerenbergh, *et al.*. Silicon microring resonators[J]. Laser Photonics Rev, 2012, 6(1): 47-73.

17 J Ding, H Chen, L Yang, *et al.*. Low-voltage, high-extinction-ratio, Mach-Zehnder silicon optical modulator for CMOS-compatible integration[J]. Opt Express, 2012, 20(3): 3209-3218.

18 Liu Yi,Tong Xiaogang,Yu Jinlong, *et al.*. All-optical switching in silicon-on-insulator serially coupled double-ring resonator based on thermal nonlinear effect[J]. Chinese J Lasers, 2013, 40(2): 0205006.

刘 毅, 仝晓刚, 于晋龙, 等. 基于热非线性效应的硅基串联双微环谐振腔全光开关[J]. 中国激光, 2013, 40(2): 0205006.

19 Minming Geng, Lianxi Jia, Lei Zhang, *et al.*. Design and fabrication of polarization-independent micro-ring resonators[J]. Chin Phys Lett., 2008, 25 (4), 1333-1335

20 B M A. Rahman, F A Fernandez, B J Davies. Review of finite element methods for microwave and optical waveguides[J]. Proceeding of IEEE, 1991, 79(10): 1442-1448.

21 P Andrew Anderson, Bradley S Schmidt, Michal Lipson. High confinement in silicon slot waveguides with sharp bends[J]. Opt Express, 2006, 14(20): 9197-9202.

22 S C Hagness, D Rafizadeh, S T Ho, *et al.*. FDTD microcavity simulations: design and experimental realization of waveguide-coupled single-mode ring and whispering-gallery-mode disk resonators[J]. J Lightwave Technol, 1997, 15(11): 2154-2165.

23 Minming Geng, Lianxi Jia, Lei Zhang, *et al.*. Four-channel reconfigurable optical add-drop multiplexer based on photonic wire waveguide[J]. Opt Express, 2009, 17(7): 5502-5516.

24 J K S Poon, J Scheuer, S Mookherjea, *et al.*. Matrix analysis of microring coupled-resonator optical waveguides[J]. Opt Express, 2004, 12(1): 90-103

25 Dong Xiaowei, Pei Li, Jian Shuisheng. Transfer matrix method for analyzing the characteristics of multiple-ring higher order microring resonators[J]. Chinese J Lasers, 2005, 32(7): 929-932.

董小伟, 裴 丽, 简水生. 传输矩阵法分析多环高阶谐振滤波器特性[J]. 中国激光, 2005, 32(7): 929-932.

26 Li Minghui, Ma Kezhen, Luo Liang, *et al.*. Influence of coupling gap on the performance of silicon-no-insulator microring resonator[J]. Chinese J Lasers, 2014, 41(6): 0610001.

李明慧, 马可贞, 骆 亮, 等. 耦合间距对绝缘体上硅微环谐振腔的性能影响[J]. 中国激光, 2014, 41(6): 0610001.

栏目编辑: 韩 峰